Dense plasma temperature equilibration in the binary collision approximation

D. O. Gericke* and M. S. Murillo
Theoretical Division, Los Alamos National Laboratory, Los Alamos, New Mexico 87545

M. Schlanges
Institut für Physik, Ernst-Moritz-Arndt-Universität Greifswald, Domstraße 10a, 17487 Greifswald, Germany

(Received 28 August 2001; published 7 March 2002)

Temperature equilibration in dense, strongly coupled plasmas has been investigated without most of the usual simplifying assumptions. A quantum kinetic approach is used that accounts for strong electron-ion collisions through an exact *T*-matrix treatment of the scattering cross section using a screened interaction. Our results reveal the accuracy of the usual Spitzer formula for Coulomb logarithms larger than about three. Moreover, a simple model based on hyperbolic orbits yields surprisingly accurate results. We also have included equation of state effects to describe realistic plasmas.

DOI: 10.1103/PhysRevE.65.036418 PACS number(s): 52.25.Kn, 52.27.Gr

I. INTRODUCTION

The physics of dense, multitemperature plasmas is of wide interest since such plasmas are easily generated during short-pulse laser matter interaction experiments [1,2]. To model the behavior of the target, especially in the relaxation phase following the laser pulse, knowledge of the energy transfer between electrons and ions is required. Such information is also needed to simulate the evolution of the fusion capsule in inertial confinement fusion scenarios. Recent experimental results indicate that the energy transfer rates (for hot electrons as well as hot ions) are much smaller than the usual Spitzer result [1–3].

The first description of temperature equilibration originates with the seminal works of Landau and Spitzer (LS approach) in which all small angle scattering contributions are summed [4,5]. Such a treatment is only appropriate for the dilute, weakly coupled plasmas that were of interest to Landau and Spitzer. Comparisons with numerical simulations for weakly to moderately coupled plasmas show either slightly too high or slightly too low relaxation rates depending on the choice of *ad hoc* cutoffs [6,7]. Starting from a generalized Fokker-Planck equation, Li and Petrasso showed that no correction terms occur up to the next order in the electron-ion interaction [8]. Therefore, they claim that the LS result is valid for Coulomb logarithms $\lambda > 2$. This condition is illustrated in Fig. 1. Additionally, lines of constant electron-ion coupling Γ_{ei}, defined by

$$\Gamma_{ei} = \frac{Z_i e^2 (4\pi n_e/3)^{1/3}}{\langle E_{kin} \rangle}, \tag{1}$$

and constant degeneracy parameters $n_e \Lambda_e^3$ are plotted. Here, the electron thermal wavelength is defined by $\Lambda_e = (2\pi\hbar^2/m_e k_B T_e)^{1/2}$, and the average kinetic energy is given by $\langle E_{kin} \rangle = 2k_B T_e/(n_e \Lambda_e^3) I_{3/2}(\mu^{ideal}/k_B T)$ ($I_{3/2}$ is the Fermi integral with the ideal chemical potential μ^{ideal}). Note that the LS, and therefore Li and Petrasso's approach, applies only in the weakly coupled regime, i.e., for $\Gamma_{ei} < 0.1$, which excludes many systems of interest. To go beyond this approach, Ohde *et al.* applied a Boltzmann-type kinetic equation including three-particle scattering to investigate temperature relaxation in a reacting hydrogen plasma [9]. With this theory, they were able to describe binary collisions as well as ionization and recombination processes including nonideality effects.

Recently Dharma-wardana and Perrot developed models that allow an energy transfer through collective modes [10]. Hazak *et al.* have shown that under certain circumstances the Fermi-golden-rule approach, which assumes small Γ_{ei}, reduces to the LS result [11]. However, coupled collective contributions are expected to be important when Γ_{ei} is large (small λ). Unfortuately, the usual Fokker-Planck approach is ill-defined for this parameter region; therefore, Dharma-wardana and Perrot were forced to compare their results with an *ad hoc* extention of the LS theory that uses an effective Coulomb logarithm [12] to account for strong binary scattering.

It is the aim of this paper to evaluate the accuracy of the *ad hoc* approach. Therefore, we abandon the Fokker-Planck

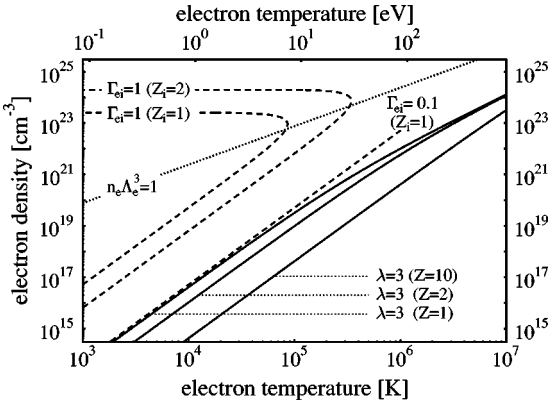

FIG. 1. Parameter region of interest, the LS theory is valid below the solid lines (our kinetic approach yields the condition $\lambda > 3$). Contours of Γ_{ei} and $n_e \Lambda_e^3$ are shown also. Note that the LS approach applies only for $\Gamma_{ei} < 0.1$.

*Electronic address: gericke@lanl.gov

TABLE I. Different approximations for the Coulomb logarithm λ.

No.	λ	b_{max}	b_{min} or b_{ref}	$\lambda<0$?	Comment
1	$\lambda=\ln(b_{max}/b_{min})$	λ_D	$(\lambda\!\!\!^{-2}+\rho_\perp^2)^{1/2}$	possible	within 5% of T-matrix result for $\lambda>3$
2	$\lambda=\ln(b_{max}/b_{min})$	$(\lambda_D^2+a_i^2)^{1/2}$	$(\lambda\!\!\!^{-2}+\rho_\perp^2)^{1/2}$	possible	improves No. 1 for high densities
3	$\lambda=\max(2,\lambda')$ [λ' as in No. 1]	λ_D	$(\lambda\!\!\!^{-2}+\rho_\perp^2)^{1/2}$	impossible	same as No. 1; no improvement for $\lambda<2$
4	$\lambda=0.5\ln(1+b_{max}^2/b_{ref}^2)$	λ_D	$(\lambda\!\!\!^{-2}+\rho_\perp^2)^{1/2}$	impossible	same as No. 1, but no breakdown
5	$\lambda=0.5\ln(1+b_{max}^2/b_{ref}^2)$	$(\lambda_D^2+a_i^2)^{1/2}$	$\rho_\perp$	impossible	overestimates λ for high temperatures
6	$\lambda=0.5\ln(1+b_{max}^2/b_{ref}^2)$	$(\lambda_D^2+a_i^2)^{1/2}$	$(\lambda\!\!\!^{-2}+\rho_\perp^2)^{1/2}$	impossible	best model; improves No. 4 for high densities

approach and use a method similar to Ohde *et al.* [9], but consider only *binary collisions*. With this description of the energy transfer, which is valid for large Γ_{ei}, strong electron-ion collisions, quantum diffraction effects, screened interactions, dynamic screening effects, and momentum dependent cross sections can be considered. In addition, we avoid any *ad hoc* cutoff procedure. The only assumptions are linearly screened Coulomb interactions, a Maxwellian distribution for the electrons, and independent ions. A comparison with this highly accurate theory then allows an experimental observation of the failure of the binary collision approximation in general, i.e., the occurrence of dominant coupled mode effects. Since we consider situations where all species have already reached a Maxwellian distribution, ultrafast relaxation effects, such as the build up of correlations and momentum relaxation, will be neglected.

II. THE CLASSICAL LANDAU-SPITZER APPROACH

A. Straight line trajectories

We briefly summarize the LS approach. With the assumption of classical small angle scattering (straight line trajectories with an impact parameter b), the time evolution of the electron temperature T_e is determined by $dT_e/dt=\Sigma_\alpha(T_\alpha-T_e)/\tau^{\alpha e}$, where the sum runs over all ion species. For the relaxation time τ^{ei} the Spitzer theory gives [5]

$$\tau^{ei}=\frac{3m_im_e}{4\sqrt{2\pi}n_iZ_i^2e^4\lambda}\left(\frac{k_BT_e}{m_e}+\frac{k_BT_i}{m_i}\right)^{3/2}, \tag{2}$$

where the index i labels ion properties. The Coulomb logarithm is here defined as $\lambda=\ln(b_{max}/b_{min})$ with the maximum and minimum impact parameters b_{max} and b_{min}, respectively. For the "usual" LS result, we will use the electron Debye length $\lambda_D=(k_BT_e/4\pi e^2n_e)^{1/2}$ for b_{max} and $b_{min}=(\lambda\!\!\!^{-2}+\rho_\perp^2)^{1/2}$, which is an interpolation between the de Broglie wavelength $\lambda\!\!\!^{-}=\hbar/2m_ev_{th}$ and the distance of closest approach $\rho_\perp=Z_ie^2/m_ev_{th}(v_{th}^2=k_BT/m_e)$. Obviously, this approach fails when $\lambda<0$, although a clamp at some λ_{min} (see No. 3 in Table I) can be used to prevent negative τ^{ei}.

B. Hyperbolic trajectories

For large Γ_{ei} the concept of straight line trajectories fails and the result (2) is invalid. However, a simple Spitzer-like theory can be constructed by noting that the shape of the trajectories are known exactly to be hyperbolic for Coulomb interactions. It follows for the energy transfer per collision that [13]

$$\Delta E(b,v)=\frac{2Z^2e^4}{m_ev^2(b^2+Z^2e^4/m_e^2v^4)}. \tag{3}$$

Here v is the relative velocity. Now b_{min} can be set to be zero since the divergence for small b is removed. The effective Coulomb logarithm, which we will refer as HLS, is then

$$\lambda=\frac{1}{2}\ln(1+(b_{max}^2/b_{ref}^2)), \tag{4}$$

where $b_{ref}=\rho_\perp$ is a reference impact parameter. However, this form still requires an *ad hoc* cutoff for b_{max}, which is again set to be λ_D. To get quantum effects approximately, $\lambda\!\!\!^{-}$ can be used in b_{ref} too. Moreover, we suggest that for dense systems, λ_D should be replaced by the ion sphere radius $a_i=(3/4\pi n_i)^{1/3}$. Since we want to recover the physics of dilute plasmas, we suggest $b_{max}=(\lambda_D^2+a_i^2)^{1/2}$. A form as in Eq. (4), which is obtained here with hyperbolic trajectories, was also proposed in Refs. [12,14] and used in Ref. [10] to get a convergent Coulomb logarithm. Table I summarizes the different approximations we use for λ.

III. QUANTUM KINETIC APPROACH

A. Strong electron-ion collisions

We now apply a quantum kinetic approach that accounts for close collisions and avoids any arbitrary cutoffs. Although this approach is quite general, we focus on the case $T_i\ll T_e$. Single-particle properties (as the kinetic energy of the species a) can be described by the distributions f_a. Since retardation effects can be neglected here, the time evolution of these distributions for systems with statically screened interactions is determined by (homogeneous, isotropic, and nondegenerate case) [15,16]

$$\frac{\partial}{\partial t}f_a(\boldsymbol{p},t)=\frac{2\pi}{V\hbar}\sum_b\int\frac{d\boldsymbol{p}'d\bar{\boldsymbol{p}}d\bar{\boldsymbol{p}}'}{(2\pi\hbar)^9}\frac{1}{2}|\langle\boldsymbol{p}\boldsymbol{p}'|T_{ab}^R|\bar{\boldsymbol{p}}'\bar{\boldsymbol{p}}\rangle^{\pm}|^2$$
$$\times\delta(E_a(\boldsymbol{p})+E_b(\boldsymbol{p})-E_a(\bar{\boldsymbol{p}})-E_b(\bar{\boldsymbol{p}}))$$
$$\times\{f_a(\bar{\boldsymbol{p}},t)f_b(\bar{\boldsymbol{p}}',t)-f_a(\boldsymbol{p},t)f_b(\boldsymbol{p}',t)\}. \tag{5}$$

The sum is over all species, but only the e-i collisions contribute to temperature equilibration. The retarded T matrix T^R_{ab} describes the transition probability from the initial to the final state. $E_a = p^2/(2m_a)$ denotes the one-particle energy. With the definition of the mean kinetic energy, i.e., $\langle E_i \rangle = (2\pi\hbar)^{-3} \int d\boldsymbol{p} E_i(p) f_i(\boldsymbol{p},t)$, we now obtain an expression for the energy transfer from the electrons to the ion subsystem or (equivalently) for the time evolution for the temperatures. Using momentum and energy conservation, two integrals in the collision integral of Eq. (5) can be performed. After transformation to the relative momentum $\boldsymbol{k}$, we introduce the differential scattering cross section for electron-ion collisions, $(2\pi)^2\hbar^4 d\sigma_{ei}(k,\Omega)/d\Omega = m_e^2 |\langle \boldsymbol{k}| T^R_{bc} |\overline{\boldsymbol{k}}\rangle|^2_{k=k}$. Finally, we get for the energy transfer rate per ion

$$\frac{\partial}{\partial t} E_i = \int \frac{d\tilde{\boldsymbol{p}}}{(2\pi\hbar)^3} \frac{f_i(\tilde{\boldsymbol{p}})}{n_i} \frac{n_e \Lambda_e^3}{(2\pi)^2 \hbar^3 m_e} \frac{k_B T_e}{\tilde{p}} \times \int_0^\infty dk\, k^3 Q^T_{ei}(k) \left[k_- e^{-\frac{m_e v_-^2}{2k_B T_e}} - k_+ e^{-\frac{m_e v_+^2}{2k_B T_e}} \right], \quad (6)$$

where the abbreviations $k_\pm = k \pm \tilde{p} + m_i k_B T_e / k$ and $v_\pm = k/m_e \pm \tilde{p}/m_i$ have been used. Furthermore, we have introduced the momentum transfer cross section $Q^T_{ei}(k) = 2\pi \int d\theta (1 - \cos\theta) d\sigma_{ei}(k,\Omega)/d\Omega$, where θ denotes the scattering angle. We calculate the cross section by a numerical phase shift analysis using the Debye potential $V_{ei}(r) = Z_i e^2 \exp(-r/\lambda_D)/r$, which is referred as the T-matrix result. The static Born result follows from Eq. (6) if Q^T_{ei} is evaluated in first Born approximation [17].

For the case $T_i \ll T_e$ the ion velocity is much smaller than the thermal electron velocity, and all terms after the ion distribution in Eq. (6) can be evaluated at $\tilde{\boldsymbol{p}} = 0$. The energy transfer rate per ion is then

$$\frac{\partial}{\partial t} E_i = \frac{1}{2\pi^2 \hbar^3} \frac{n_e \Lambda_e^3}{m_e m_i} \int_0^\infty dk\, k^5 Q^T_{ei}(k) \exp\left(- \frac{k^2}{m_e k_B T_e} \right). \quad (7)$$

This expression describes the temperature relaxation due to binary collisions for large Γ_{ei} without *ad hoc* cutoffs.

B. Dynamic screening effects

We estimate the importance of dynamic screening effects with the Lenard-Balescu equation, instead of the Boltzmann equation (5), which yields for $T_i \ll T_e$

$$\frac{\partial}{\partial t} E_i = \frac{4 Z_i^2 e^2}{\pi} \int_0^\infty dk \frac{\hbar k^2}{2m_i} \mathrm{Im} \left[\varepsilon^{-1} \left(k, \frac{\hbar k^2}{2m_i} \right) \right] n_B \left(\frac{\hbar k^2}{2m_i} \right). \quad (8)$$

Here $n_B(\omega) = [\exp(\omega/k_B T_e) - 1]^{-1}$ is the Bose function and $\varepsilon(k,\omega)$ is the dielectric function computed in the random phase approximation. Equation (8) is similar to the self-energy approach of Dharma-wardana and Perrot [10]. Dynamic screening effects can be approximately included in the T-matrix approach by summing the expressions (7) and (8) and subtracting the statically screened first Born approximation [18] (combined approach).

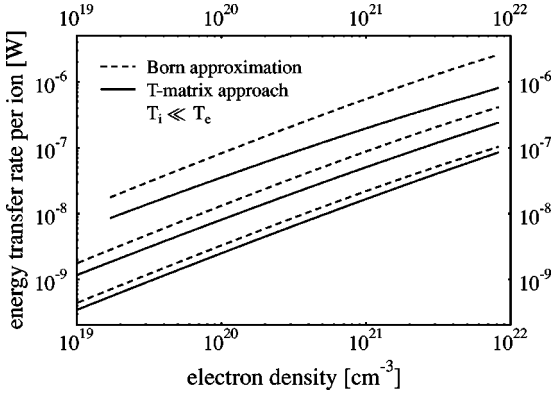

FIG. 2. Comparison of the first Born and the T-matrix results for the energy transfer rate in an aluminum plasma. The lines belong to three different charged states of the ions, $Z_i = 1$ (lower pair of lines), $Z_i = 2$ (middle pair), and $Z_i = 7$ (upper pair). The electron temperature is $T_e = 10^5$ K.

IV. RESULTS AND DISCUSSION

A. Comparison of the different approaches

A comparison of the first Born and T-matrix results is shown in Fig. 2 for different charge states of the ions, which were assumed to be fixed as the density is varied. The lines end where degeneracy effects are expected, i.e., for $n_e \Lambda_e^3 > 0.1$. The Born approximation always overestimates the energy transfer rate. Although this effect is quite small for singly charged ions, it strongly increases for higher charge states (in general, it increases for stronger electron-ion coupling). This is a result of the different scaling laws, the Born results scale as Z_i^2 whereas, the T-matrix calculation yields a smaller scaling exponent.

The effect of dynamical screening is demonstrated in Fig. 3, where different approximation levels for the energy transfer rate are shown. Only very small differences can be ob-

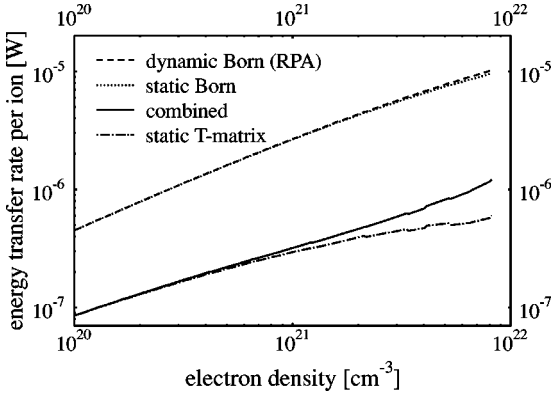

FIG. 3. Effect of dynamic screening in the Born and T-matrix approximations. Results are shown for an aluminum plasma with an electron temperature of $T_e = 5 \times 10^4$ K. The ion charge state is fixed to be $Z_i = 11$.

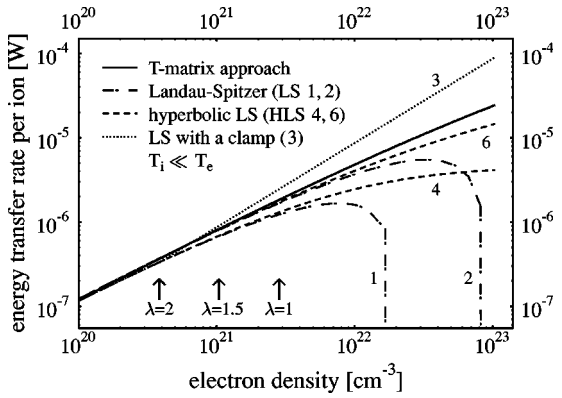

FIG. 4. Comparison of different Spitzer approximations with the *T*-matrix approach. The system has an electron temperature of $T_e = 5\times10^5$ K. The ion charge state is $Z_i = 10$. The numbers next to the lines refer to Table I.

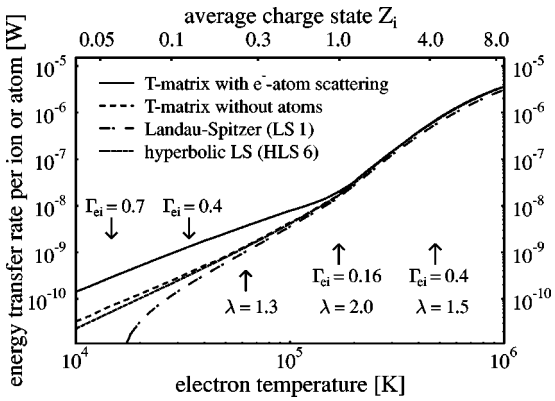

FIG. 5. Energy transfer rate vs temperature for an aluminum plasma with a nuclear density of $n = 10^{21}$ cm^{-3}. The chemical composition is calculated using a Thomas-Fermi equation of state model.

served between the dynamic and the static Born approximation (upper pair of lines) for high densities (strong coupling). This behavior suggests that dynamic screening effects are negligible. However, the Born approximation strongly overestimates the energy transfer rate in this regime. Since the combined scheme is the difference between the static and dynamic Born results added to the (much smaller) static *T*-matrix data, the effect of dynamic screening can be significant on the *T*-matrix level. Comparing the lower two lines in Fig. 3, i.e., the static *T*-matrix approach with the combined scheme, this behavior can be observed at high densities. However, these dynamic screening effects quickly disappear for smaller Γ_{ei}, i.e., they appear only for extremely high (nonequilibrium) charge states of the ions.

In Fig. 4 the different models for the LS and HLS energy transfer rate are compared with the *T*-matrix approach. Of course, the LS theory (Nos. 1 and 2) is undefined for nonideal plasmas since $\lambda < 0$ in this case. The clamp technique (No. 3) avoids this behavior but overestimates the rate for $\lambda < 2$. Only the HLS approaches (Nos. 4 and 6) show a reasonable behavior without a breakdown. However, they still underestimate the energy transfer for strongly coupled plasmas. Note that the choice $b_{max} = (\lambda_D^2 + a_i^2)^{1/2}$ greatly improves the LS and the HLS theories.

To explore the pure influence of the Coulomb cutoff in contrast to the screened Coulomb potential, we calculated the energy transfer rate with Eq. (7) using a cross section, which was calculated with hyperbolic orbits for a truncated Coulomb potential (cutoff at $b_{max} = \lambda_D$). In this way, we include an average over the distribution. The results, which are not shown in the figure, are very close to the line labeled with No. 6. This shows that an integration over the distribution, rather than simply using the thermal velocity, improves the theory (compare with No. 4). The remaining discrepancies to the *T*-matrix results are due to the different potentials.

There are three major conclusions from this comparison. We have confirmed Li and Petrasso's claim that there are small corrections to the LS result for many conditions, although we would give $\lambda = 3$ (corrections less than 5%), rather than $\lambda = 2$, as a boundary. Second, the simple HLS model goes well beyond the Fokker-Planck approaches and is accurate as long as a classical trajectory is well defined. This is especially surprising because an angular momentum-truncated Coulomb potential is used in the LS and HLS calculations, rather than a screened Coulomb potential. Finally, the *T*-matrix approach yields rates larger than the LS and HLS theories for large Γ_{ei}. Thus, the effect of coupled collective modes [10] may be larger than previously believed.

Since the numerical *T*-matrix calculations are time expensive, we provide a fit. We chose a model where the relaxation time is determined by Eq. (2) with λ given by the HLS theory (4). The free parameter of this theory b_{max} has been determined by the constraint that the HLS theory matches the *T*-matrix results. We obtain

$$b_{max} = \lambda_D \exp\left(\frac{a_1 + a_2 \ln\lambda}{\lambda^{a_3} + 1}\right), \tag{9}$$

where λ is the HLS Coulomb logarithm (see Table I, No. 4), $a_1 = 1.65$, $a_2 = -0.40$, and $a_3 = 0.64$. For nondegenerate plasmas ($n_e \Lambda_e^3 < 0.1$), this fit yields energy transfer rates within 15% for $\lambda > 2\times10^{-2}$, and for $\lambda > 5\times10^{-3}$, the errors are smaller than 30%. For larger λ the fit is significantly more accurate. Note that $b_{max} \geqslant \lambda_D$.

B. Effects of plasma composition

Finally, we consider the chemical composition of the plasma. The average charge state $Z_i(n, T_e)$ is calculated with the Thomas-Fermi model of More [19]. For mean charge states less than unity, elastic electron-atom scattering is included with a three-particle collision integral [15]. To model the electron-atom interaction, we use the screened polarization potential [17]

$$V_{ea}^P(r) = -\frac{e^2\alpha}{2}\left(\frac{1 + r/\lambda_D}{(r^2 + r_0^2)}\right)^2 \exp\left[-\frac{2r}{\lambda_D}\right]. \tag{10}$$

The polarizability for aluminum atoms is $\alpha = 56.28 a_B^3$, and with $r_0^4 = \alpha a_B / 2 Z_c^{1/3}$ [20], it follows $r_0 = 1.86 a_B$.

Figure 5 shows the energy transfer rate for a fixed nuclear

density versus temperature. The largest differences between the models occur for low temperatures, in particular, the LS approach is not well defined and does not include electron-atom scattering. We also show *T*-matrix results neglecting electron-atom scattering, but deviations from the LS and HLS results are also found for the pure electron-ion contribution. A disagreement is visible for higher temperatures too. In contrast, there is a good agreement for temperatures near $T_e = 2 \times 10^5$ K. This behavior results because, as the plasma parameters change, the electron-ion coupling is large for small temperatures and decreases up to the point where multiply charged ions occur. Above this temperature, the increasing charge state and electron density overcompensate the effect of the increasing temperature, which increases the electron-ion coupling strength again. Of course, the charge state and the electron density show a saturation for high enough temperatures (not shown). Above this temperature, the plasma becomes again weakly coupled and all approximations merge. Qualitatively, the Coulomb logarithm shows a similar behavior to Γ_{ei} (increasing λ up to $T_e \approx 10^5$ K and then again decreasing), which results in the inapplicability of the Spitzer approach.

ACKNOWLEDGMENTS

This work was supported by the United States Department of Energy and the Deutsche Forschungsgemeinschaft (Sonderforschungsbereich 198). D.G. thanks the German Academic Exchange Service (DAAD).

[1] P. Celliers, A. Ng, G. Xu, and A. Forsman, Phys. Rev. Lett. **68**, 2305 (1992).
[2] A. Ng, P. Celliers, G. Xu, and A. Forsman, Phys. Rev. E **52**, 4299 (1995).
[3] D. Riley, N.C. Woolsey, D. McSherry, I. Weaver, A. Djaoui, and E. Nardi, Phys. Rev. Lett. **84**, 1704 (2000).
[4] L.D. Landau, Phys. Z. Sowjetunion **10**, 154 (1936) [JETP **7**, 203 (1937)].
[5] L. Spitzer, *Physics of Fully Ionized Gases* (Interscience, New York, 1967).
[6] J.C. Hansen and I.R. McDonald, Phys. Lett. **97A**, 42 (1983).
[7] U. Reimann and C. Toepffer, Laser Part. Beams **8**, 771 (1990).
[8] C.-K. Li and R.D. Petrasso, Phys. Rev. Lett. **70**, 3063 (1993).
[9] Th. Ohde, M. Bonitz, Th. Bornath, D. Kremp, and M. Schlanges, Phys. Plasmas **3**, 1241 (1996).
[10] M.W.C. Dharma-wardana and F. Perrot, Phys. Rev. E **58**, 3705 (1998); **63**, 069901 (2001).
[11] G. Hazak, Z. Zinamon, Y. Rosenfeld, and M.W.C. Dharma-wardana, Phys. Rev. E **64**, 066411 (2001).
[12] Y.T. Lee and R.M. More, Phys. Fluids **27**, 1273 (1984).
[13] J.D. Jackson, *Classical Electrodynamics* (Wiley, New York, 1975).
[14] R. Cauble and W. Rozmus, Phys. Rev. E **52**, 2974 (1995).
[15] Y.L. Klimontovich and D. Kremp, Physica A **109**, 517 (1981).
[16] P. Danielewicz, Ann. Phys. (N.Y.) **152**, 239 (1984).
[17] W. Ebeling *et al.*, *Transport Properties of Dense Plasmas* (Akademie-Verlag, Berlin, 1983).
[18] D.O. Gericke, M. Schlanges, and W.D. Kraeft, Phys. Lett. A **222**, 241 (1996).
[19] R. M. More, in *Advances in Atomic and Molecular Physics*, edited by D. Bates and B. Bederson (Academic, New York, 1985), Vol. 21.
[20] M.H. Mittleman and K.M. Watson, Phys. Rev. **113**, 198 (1959).